

# ***Supporting Information For***

## **Molecular insights into hybrid CH<sub>4</sub> physisorption-hydrate formation in spiral halloysite nanotubes: Implications for energy storage**

Fengyi Mi<sup>†,‡</sup>, Zhongjin He<sup>\*,†</sup>, Jiangtao Pang<sup>†</sup>, Othonas A. Moultos<sup>‡</sup>, Thijs J.H. Vlugt<sup>‡</sup>, Fulong Ning<sup>†</sup>

<sup>†</sup>National Center for International Research on Deep Earth Drilling and Resource Development, Faculty of Engineering, China University of Geosciences, Wuhan, Hubei 430074, China

<sup>‡</sup>Engineering Thermodynamics, Process & Energy Department, Faculty of Mechanical Engineering, Delft University of Technology, Leeghwaterstraat 39, Delft, 2628CB, the Netherlands

\*Authors to whom correspondence should be addressed. [hezhongjin@cug.edu.cn](mailto:hezhongjin@cug.edu.cn)

Total number of pages: 21

Total number of figures: 26

Total number of tables: 2

Total number of videos: 6

## Contents of Supporting Information

### Additional Methods

### Supporting Tables

Table S1. Parameters for the three simulation systems for CH<sub>4</sub> storage.

Table S2. Parameters for the force field.

### Calculation of the diffusion coefficient ( $K_{DC}$ )

### Calculation of the distance between hydrate and HNTs (HHD)

### Calculation of the conversion ratio

### Additional Results and Discussions

### Supporting Figures

Figure S1. The schematic diagram of the final simulation model for the (a) R<sub>0.08</sub>, (b) R<sub>0.12</sub>, and (c) R<sub>0.148</sub> simulation systems.

Figure S2. The adsorption processes of CH<sub>4</sub> molecules inside and outside of the HNTs in the (a-c) R<sub>0.08</sub> and (d-f) R<sub>0.148</sub> simulation systems. Green balls represent CH<sub>4</sub> molecules. The HNTs are displayed as polyhedral, *i.e.* yellow (Si atom) and pink (Al atom).

Figure S3. The evolution of the number of CH<sub>4</sub>/H<sub>2</sub>O molecules for different distances from the inner and outer surfaces of the HNTs for the (a-d) R<sub>0.148</sub>, (e-h) R<sub>0.12</sub>, and (i-l) R<sub>0.08</sub> simulation systems.

Figure S4. The number of CH<sub>4</sub>/H<sub>2</sub>O molecules under different distances from the inner and outer surfaces of the HNTs at the end of 20-ns adsorption simulation for the (a-b) R<sub>0.148</sub> and (c-d) R<sub>0.08</sub> simulation systems.

Figure S5. The evolution of the number of CH<sub>4</sub> adsorbed on the outer surface and of the proportion of CH<sub>4</sub>/H<sub>2</sub>O molecules inside of the HNTs during 20-ns adsorption simulation for the (a) R<sub>0.148</sub> and (b) R<sub>0.08</sub> simulation systems.

Figure S6. The evolution of the number of CH<sub>4</sub>/H<sub>2</sub>O molecules inside and outside of the HNTs for the (a) R<sub>0.148</sub>, (b) R<sub>0.12</sub>, and (c) R<sub>0.08</sub> systems for adsorption simulation.

Figure S7. Diffusion coefficients ( $K_{DC}$ ) of CH<sub>4</sub>/H<sub>2</sub>O molecules under different distances from the inner and outer surfaces of the HNTs at the end of 20-ns adsorption simulation for the (a, b) R<sub>0.148</sub> and (c, d) R<sub>0.08</sub> systems.

Figure S8. Formation processes of CH<sub>4</sub> hydrate inside and outside of the HNTs for the (a-i) R<sub>0.08</sub> system.

Figure S9. Formation processes of CH<sub>4</sub> hydrate inside and outside of the HNTs for the (a-i) R<sub>0.148</sub> system.

Figure S10. Number density distribution of CH<sub>4</sub> molecules for the last 0.001  $\mu$ s in the three simulation systems *i.e.* (a-c) R<sub>0.08</sub>, (d-f) R<sub>0.12</sub>, (g-i) R<sub>0.148</sub> simulation systems.

Figure S11. The evolution of the (a-b) conversion ratio of CH<sub>4</sub>/H<sub>2</sub>O molecules and (c-d) number of CH<sub>4</sub>/H<sub>2</sub>O molecules in solution and hydrate inside and outside of the HNTs for the R<sub>0.08</sub> simulation system.

Figure S12. The evolution of the (a-b) conversion ratio of CH<sub>4</sub>/H<sub>2</sub>O molecules and (c-d) number of CH<sub>4</sub>/H<sub>2</sub>O molecules in solution and hydrate inside and outside of the HNTs for the R<sub>0.148</sub> simulation system.

Figure S13. The evolution of the number of (a) H<sub>2</sub>O and (b) CH<sub>4</sub> molecules in solution and hydrate for the R<sub>0.12</sub> simulation system.

Figure S14. The evolution of the number of hydrogen bonds between water molecules and both the inner and outer surfaces of the HNTs for the (a) R<sub>0.148</sub>, (b) R<sub>0.12</sub>, and (c) R<sub>0.08</sub> simulation systems.

Figure S15. The evolution of the CH<sub>4</sub> mole fraction in water  $x_{\text{CH}_4}$  inside and outside of the HNTs and total for the (a) R<sub>0.148</sub>, (b) R<sub>0.12</sub>, and (c) R<sub>0.08</sub> simulation systems.

Figure S16. The evolution of the CH<sub>4</sub> in the nanobubbles  $N_{\text{CH}_4}$  inside and outside of the HNTs and total for the (a) R<sub>0.148</sub>, (b) R<sub>0.12</sub>, and (c) R<sub>0.08</sub> simulation systems.

Figure S17. The evolution of the number of CH<sub>4</sub>/H<sub>2</sub>O molecules migration from inside to outside of the HNTs for the (a) R<sub>0.08</sub>, (b) R<sub>0.12</sub>, and (c) R<sub>0.148</sub> simulation systems.

Figure S18. The evolution of the  $F_4$  order parameter under the different distances from the inner and outer surfaces of the HNTs for the (a, d) R<sub>0.148</sub>, (b, e) R<sub>0.12</sub>, and (c, f) R<sub>0.08</sub> simulation systems.

Figure S19. The evolution of the number of CH<sub>4</sub>/H<sub>2</sub>O molecules in hydrate under the different distances from the inner and outer surfaces of the HNTs for the (a-d) R<sub>0.148</sub>, (e-h) R<sub>0.12</sub>, and (i-l) R<sub>0.08</sub> simulation systems.

Figure S20. The snapshot of the hydrogen bonds (green lines) between the bound water on the inner surface and the hydrate solids inside of the HNTs at 2.0-μs for the (a-i) R<sub>0.08</sub> simulation system.

Figure S21. The evolution of the diffusion coefficient ( $K_{\text{DC}}$ ) of CH<sub>4</sub>/H<sub>2</sub>O molecules as a function of the radial distances from the inner and outer surfaces of the HNTs for the (a-d) R<sub>0.148</sub>, (e, h) R<sub>0.12</sub>, and (i-l) R<sub>0.08</sub> systems.

Figure S22. The evolution of the solvent accessible surface area of CH<sub>4</sub> nanobubbles for free, contact and total area in the (a) R<sub>0.08</sub>, (b) R<sub>0.12</sub>, and (c) R<sub>0.148</sub> simulation systems.

Figure S23. The evolution of the number of hydrate cages inside and outside of the HNTs for the (a) R<sub>0.08</sub>, (b) R<sub>0.12</sub>, and (c) R<sub>0.148</sub> simulation systems.

Figure S24. The evolution of the  $F_4$  order parameter for the R<sub>0.148</sub>, R<sub>0.12</sub>, and R<sub>0.08</sub> simulation systems.

Figure S25. Snapshots of water ring inside and outside of the HNTs at 2 μs (a-c) in the R<sub>0.08</sub>, R<sub>0.12</sub> and R<sub>0.148</sub> simulation systems. Cyan, red, blue and orange balls represent ring\_4, ring\_5, ring\_6 and ring\_7, respectively.

Figure S26. The evolution of the number of hydrate cages for the (a) R<sub>0.08</sub>, (b) R<sub>0.12</sub>, and (c) R<sub>0.148</sub> simulation systems.

## Supporting Videos

Video S1-S3. Adsorption processes of CH<sub>4</sub> molecules inside and outside of the HNTs for the R<sub>0.08</sub>, R<sub>0.12</sub> and R<sub>0.148</sub> simulation systems, respectively.

Video S4-S6. Formation processes of CH<sub>4</sub> hydrates inside and outside of the HNTs for the R<sub>0.08</sub>, R<sub>0.12</sub> and R<sub>0.148</sub> simulation systems, respectively.

## Supporting Reference

## Additional Methods

The Halloysite nanotube (HNTs) has a unique structure, featuring the hydrophobic siloxane on its outer surface and the hydrophilic gibbsite on its inner lumen surface.<sup>1, 2</sup> The outer surface of the HNTs can adsorb CH<sub>4</sub> molecules. At the same time, an abundant relatively confined space will be formed between the HNTs. In the confined space, CH<sub>4</sub> molecules adsorbed on the outer surface of the HNTs can be trapped through physisorption. The hydrophilic inner surface of the HNTs can adsorb a large number of water molecules, and the presence of these water molecules provides a sufficient water source for hydrate formation inside of the HNTs.<sup>3</sup> In this study, CH<sub>4</sub> and water molecules can freely exchange between inside and outside of the HNTs. The mole fraction of CH<sub>4</sub> inside and outside of the HNTs was set to the same value, eliminating the impact of the initial configuration on the migration of CH<sub>4</sub> inside and outside the halloysite. The detailed force field parameters for H<sub>2</sub>O, CH<sub>4</sub>, and HNT in the system are shown in Table S2. To explore the physisorption processes of CH<sub>4</sub> molecules on the surface of the HNTs, a 20-ns adsorption simulation was performed under the isothermal-isobaric (*NPT*) ensemble. The temperature of 300 K is controlled by the velocity-rescaling thermostat,<sup>4</sup> and the pressure of 10 MPa is controlled by the Berendsen barostat.<sup>5</sup>

**Table S1.** Parameters for the three simulation systems for CH<sub>4</sub> storage.

Pressure in the three simulation systems: 10 MPa					
System	Simulation	<i>N</i> <sub>CH<sub>4</sub></sub>	<i>N</i> <sub>H<sub>2</sub>O</sub>	Temperature	Simulation Time
$R_{0.08}$	Adsorption	2260	25986	300 K	20 ns
	Hydrate-formation	2260	25986	240 K	2.0 $\mu$ s
$R_{0.12}$	Adsorption	3390	24856	300 K	20 ns
	Hydrate-formation	3390	24856	240 K	2.0 $\mu$ s
$R_{0.148}$	Adsorption	4184	24062	300 K	20 ns
	Hydrate-formation	4184	24062	240 K	2.0 $\mu$ s

**Table S2.** Parameters for the TIP4P/ice water model,<sup>6</sup> OPLS-UA methane,<sup>7</sup> and the CLAYFF force field.<sup>8</sup>  $\sigma$  and  $\varepsilon$  are the Lennard-Jones parameters, in units of nm and kJ/mol, respectively;  $q$  is the partial charge of an atom in units of elementary charge (e);  $m$  is the atomic mass in units of g/mol.

atom	$\varepsilon$ / [kJ/mol]	$\sigma$ / [nm]	$q$ / [e]	$m$ / [g/mol]
H <sub>2</sub> O				
O (MW)	0	0	-1.1794	0
O	0.8822	0.31668	0	16
H	0	0	0.5897	1.008
CH <sub>4</sub>	1.23	0.373	0	16
Halloysite				
Si (st)	$7.70065 \times 10^{-6}$	0.3302	2.1	28.09
Al (ao)	$5.56388 \times 10^{-6}$	0.4271	1.575	26.98
O (ob)	0.65017	0.316556	-1.05	16
O (oh)	0.65017	0.316556	-0.95	16
H (ho)	0	0	0.425	1.008

### Calculation of the diffusion coefficient ( $K_{DC}$ )

Mean square displacement (MSD) and diffusion coefficient  $K_{DC}$  are calculated by the program *gmx\_mpi msd* in GROMACS manual 5.0.7. Normally an index file containing atom numbers is used and the MSD is averaged over these atoms. For water molecules consisting of more than one atom,  $r_i$  can be taken as the O atom.

$$K_{DC} = \frac{\lim_{t \rightarrow \infty} \langle \|r_i(t) - r_i(0)\|^2 \rangle_{i \in A}}{6\Delta t} \quad (1)$$

In this study, each MSD is calculated within 1 ns for methane molecules and water molecules. Therefore, each diffusion coefficient is the average value within each 1 ns period.

### Calculation of the distance between hydrate and HNTs (HHD)

To reveal the positional relationship between hydrate solids and HNTs, we define a parameter HBD, which is the distance between hydrates (comprising CH<sub>4</sub> and H<sub>2</sub>O molecules) and HNTs surfaces. CH<sub>4</sub> hydrate is composed of CH<sub>4</sub> and H<sub>2</sub>O molecules. We first select each CH<sub>4</sub> molecule or H<sub>2</sub>O molecule that forms a hydrate and then calculate the distance between each atom in the HNTs surfaces and the hydrate (the CH<sub>4</sub> molecule or H<sub>2</sub>O molecule). The minimum value is the distance between the CH<sub>4</sub> molecules or H<sub>2</sub>O molecules in the hydrate and the HNTs surfaces.

$$HBD \in \{D_1, D_2, D_3, D_4 \dots\}_{min} \quad (2)$$

Where  $D_1$  is the distance between the CH<sub>4</sub> or H<sub>2</sub>O molecule and an atom in the HNTs surfaces.  $D_2$  is the distance between the CH<sub>4</sub> or H<sub>2</sub>O molecule and another atom in the HNTs surfaces. We count all distance values and only take the minimum value.

### Calculation of the conversion ratio

We define the conversion ratio. CH<sub>4</sub> hydrate is composed of CH<sub>4</sub> and H<sub>2</sub>O molecules. Conversion ratio is defined as the number of CH<sub>4</sub>/H<sub>2</sub>O in hydrate divided by the total number.

$$\text{Conversion ratio} = \frac{N_{\text{Hydrate}}}{N_{\text{total}}} \quad (3)$$

Where  $N_{\text{Hydrate}}$  is the number of the CH<sub>4</sub> or H<sub>2</sub>O molecule formed hydrate.  $N_{\text{total}}$  is the total number of the CH<sub>4</sub> or H<sub>2</sub>O in the system. In this study, each conversion ratio is calculated within 1 ns for CH<sub>4</sub> or H<sub>2</sub>O molecules. Therefore, each conversion ratio is the average value within each 1 ns period.

### Additional Results and Discussions

In adsorption simulations, the inner and outer surfaces of the HNTs exhibit different affinities for CH<sub>4</sub>/H<sub>2</sub>O molecules. Outside of the HNTs, CH<sub>4</sub> molecules will quickly form an obvious wave peak on the outer surface of the HNTs, while H<sub>2</sub>O molecules will form a relatively flat wave peak on the outer surface of the HNTs (Figure S3). This indicates that the outer surface of the HNTs has a strong affinity for CH<sub>4</sub> molecules and a weak affinity for H<sub>2</sub>O molecules. Inside of the HNTs, CH<sub>4</sub> molecules form small wave peaks farther away from the inner surface, while H<sub>2</sub>O molecules can form obvious peaks near the inner surface (Figure S3). This shows that the inner surface of the HNTs can strongly adsorb H<sub>2</sub>O molecules and repel CH<sub>4</sub> molecules. The adsorption process occurs in a short time. During the period of 1 - 20 ns, the number of adsorbed CH<sub>4</sub> and H<sub>2</sub>O molecules on the inner and outer surfaces of the HNTs changes little.

We pre-filled the inner and outer regions of the HNTs with a homogeneous CH<sub>4</sub> solution, which skips the initial diffusion process that would typically occur in a real system. This setup leads to a different mass transfer pattern (Figure S5(a-b)). Moreover, the CH<sub>4</sub> solution in the simulation is supersaturated, resulting in the rapid formation of CH<sub>4</sub> nanobubbles. This rapid nanobubble formation significantly affects the mass transfer of CH<sub>4</sub> and H<sub>2</sub>O molecules. In a real system, the hydrophilic inner surface would indeed attract more H<sub>2</sub>O molecules, and the hydrophobic outer surface would promote CH<sub>4</sub> adsorption. The dynamics observed in the simulation are strongly influenced by the pre-filled setup and supersaturated CH<sub>4</sub> solution, which temporarily alters the expected diffusion

behavior.

In the  $R_{0.08}$  simulation system, due to the low gas-water ratio, a large number of  $\text{CH}_4$  molecules can be converted into hydrates. Conversion ratio is defined as the number of  $\text{CH}_4/\text{H}_2\text{O}$  in hydrate divided by the total number. The conversion ratio of  $\text{CH}_4$  molecules inside and outside of the HNTs is high (Figure S11). Likewise,  $\text{CH}_4$  hydrate formation also means that a large number of  $\text{H}_2\text{O}$  molecules participate in hydrate formation. Hence, the conversion ratio of  $\text{H}_2\text{O}$  molecules inside and outside of the HNTs also maintains a high value. In contrast, in the  $R_{0.148}$  system, a large number of  $\text{CH}_4$  molecules cannot be converted into hydrates immediately due to the high gas-water ratio, resulting in a low conversion ratio of  $\text{CH}_4$  molecules, especially inside of the HNTs (Figure S12).

Figure S17(a-c) shows the evolution of the number of  $\text{CH}_4/\text{H}_2\text{O}$  molecules migrating from the inside to the outside of the HNTs. It is found that the migration number of  $\text{CH}_4$  and  $\text{H}_2\text{O}$  molecules inside and outside of the HNTs is small, indicating that the mass transfer of  $\text{CH}_4/\text{H}_2\text{O}$  molecules inside and outside of the HNTs exhibits no significant variation. In the  $R_{0.08}$  and  $R_{0.12}$  simulation systems, the migration direction of  $\text{CH}_4$  molecules is from the outside to the inside of the HNTs, while the migration direction of  $\text{H}_2\text{O}$  molecules is from the inside to the outside of the HNTs (Figure S17(a-b)). In the  $R_{0.148}$  simulation system, the migration direction of  $\text{CH}_4$  molecules is from the inside to the outside of the HNTs, while the migration direction of  $\text{H}_2\text{O}$  molecules is from the outside to the inside of the HNTs (Figure S17(c)). There are different initial trends between Figure S17(a), (b), and (c). The initial difference observed in Figure S17(c) can be attributed to the higher  $\text{CH}_4$  concentration (0.148) in the  $R_{0.148}$  system. At high  $\text{CH}_4$  concentrations,  $\text{CH}_4$  nanobubbles form more rapidly inside the HNTs, which significantly influences the initial mass transfer process. The quick aggregation of  $\text{CH}_4$  molecules into nanobubbles alters the diffusion dynamics of  $\text{CH}_4/\text{H}_2\text{O}$  molecules, causing the migration pattern of  $\text{CH}_4/\text{H}_2\text{O}$  molecules to differ from the patterns seen at lower concentrations, as shown in Figure S17(a-b). However, once the nanobubbles stabilize, the overall trend becomes consistent with the other systems. *i.e.*, a few  $\text{H}_2\text{O}$  molecules migrate from inside to outside of the HNTs, while a small number of  $\text{CH}_4$  molecules diffuse in the opposite direction.

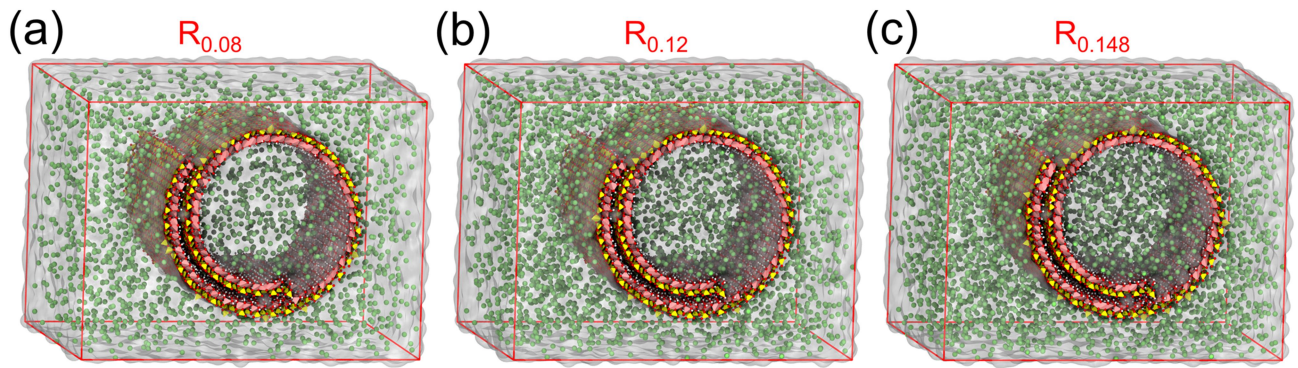


**Figure S1.** The schematic diagram of the final simulation model for the (a)  $R_{0.08}$ , (b)  $R_{0.12}$ , and (c)  $R_{0.148}$  simulation systems.

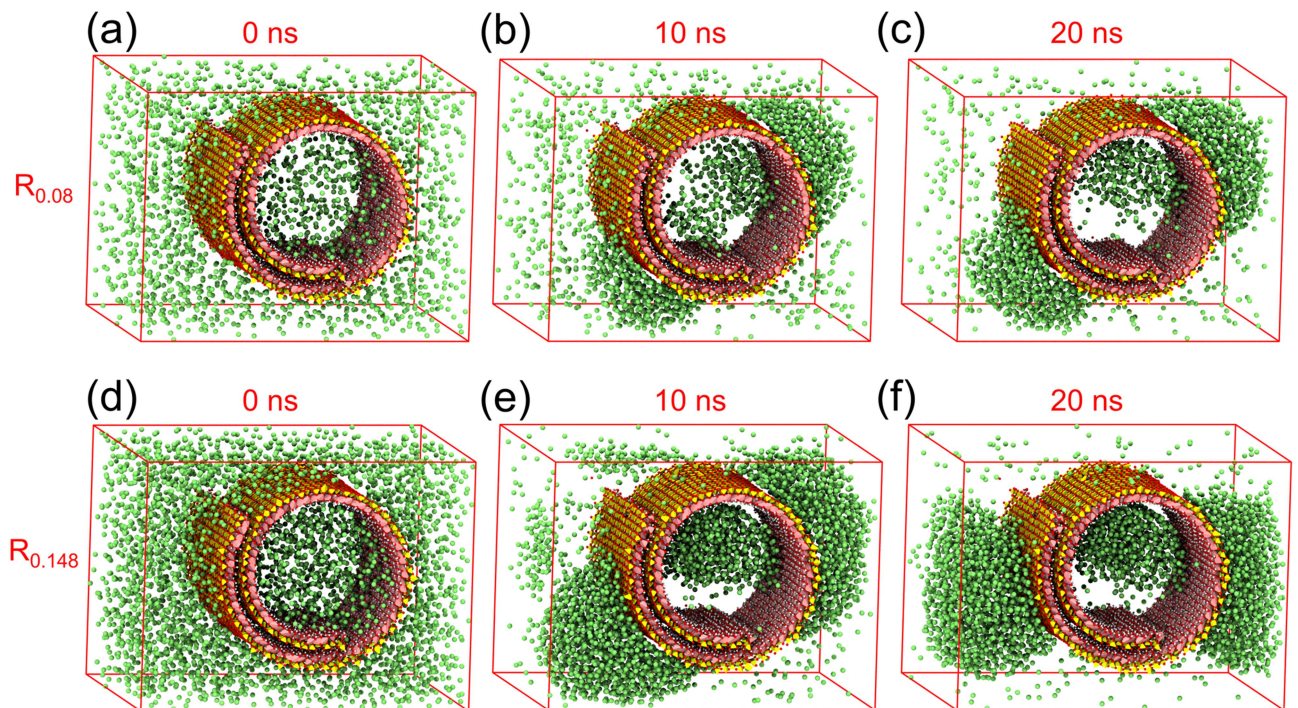


**Figure S2.** The adsorption processes of  $\text{CH}_4$  molecules inside and outside of the HNTs in the (a-c)  $R_{0.08}$  and (d-f)  $R_{0.148}$  simulation systems. Green balls represent  $\text{CH}_4$  molecules. The HNTs are displayed as polyhedral, *i.e.* yellow (Si atom) and pink (Al atom).

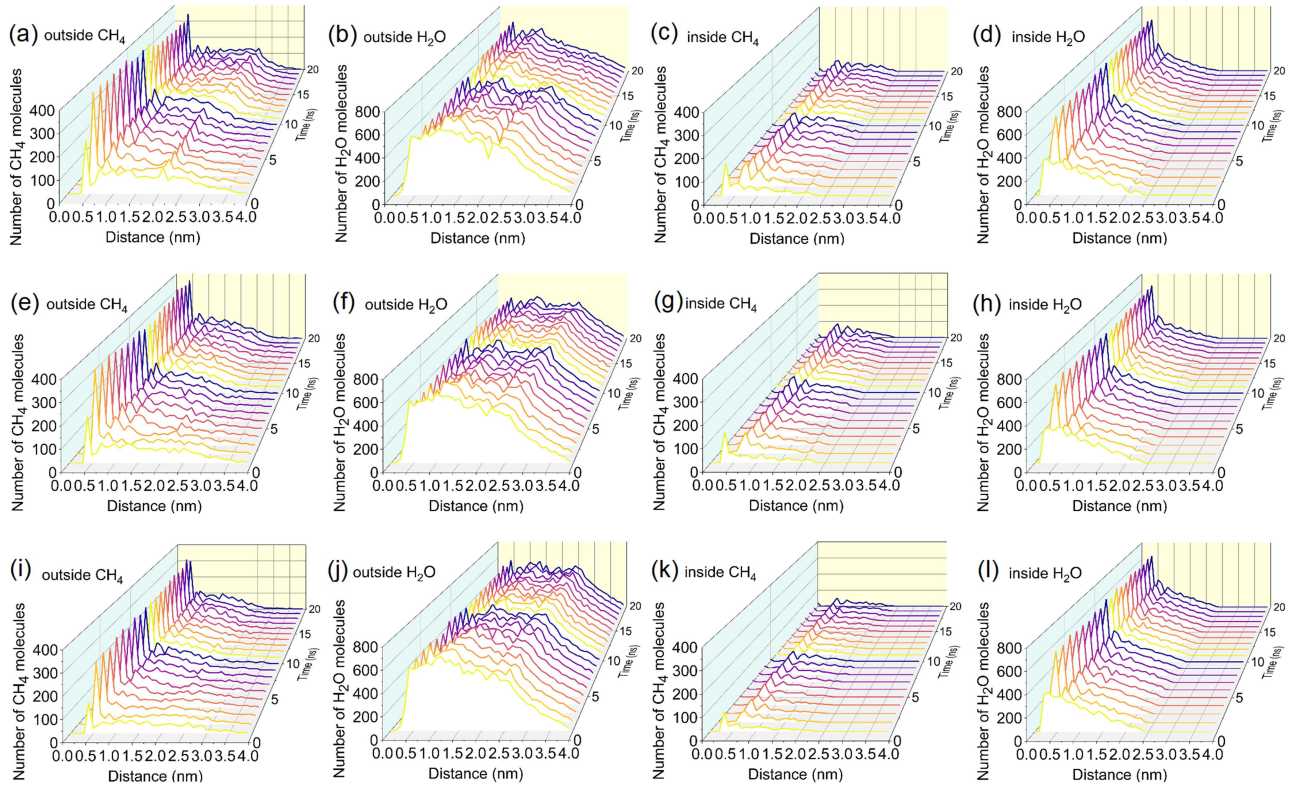


**Figure S3.** The evolution of the number of CH<sub>4</sub>/H<sub>2</sub>O molecules for different distances from the inner and outer surfaces of the HNTs for the (a-d) R<sub>0.148</sub>, (e-h) R<sub>0.12</sub>, and (i-l) R<sub>0.08</sub> simulation systems.

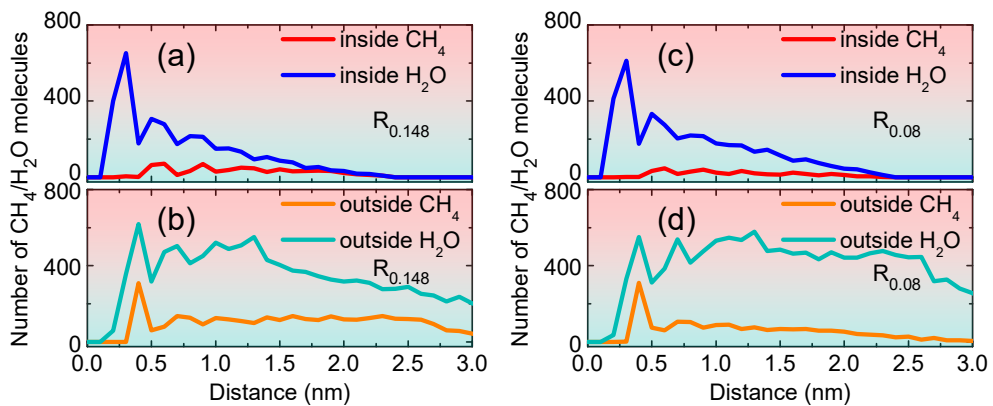


**Figure S4.** The number of CH<sub>4</sub>/H<sub>2</sub>O molecules at various radial distances from the inner and outer surfaces of the HNTs at the end of 20-ns adsorption simulation for the (a-b) R<sub>0.148</sub> and (c-d) R<sub>0.08</sub> simulation systems.

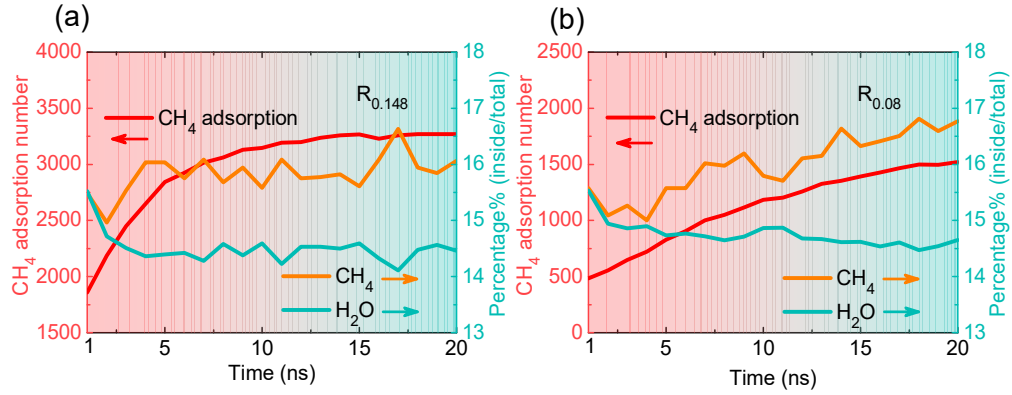


**Figure S5.** The evolution of the number of  $\text{CH}_4$  adsorbed on the outer surface and the percentage of  $\text{CH}_4/\text{H}_2\text{O}$  molecules inside of the HNTs relative to the total number of  $\text{CH}_4/\text{H}_2\text{O}$  molecules during 20-ns adsorption simulation for the (a)  $R_{0.148}$  and (b)  $R_{0.08}$  simulation systems.

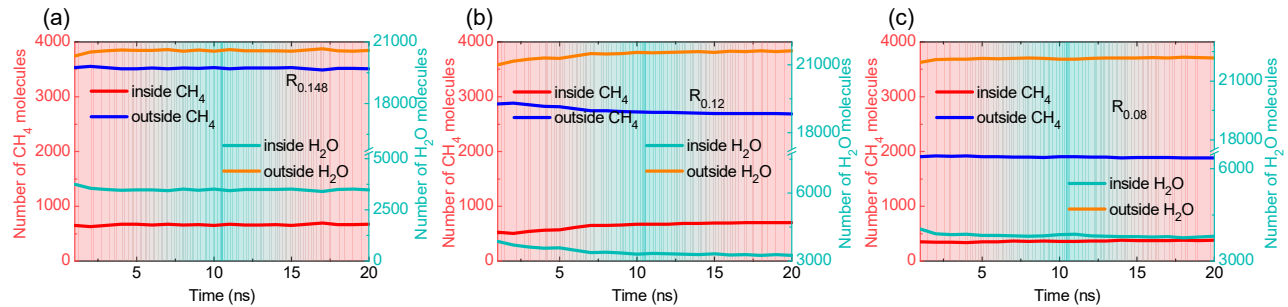


**Figure S6.** The evolution of the number of  $\text{CH}_4/\text{H}_2\text{O}$  molecules inside and outside of the HNTs for the (a)  $R_{0.148}$ , (b)  $R_{0.12}$ , and (c)  $R_{0.08}$  systems for adsorption simulation.

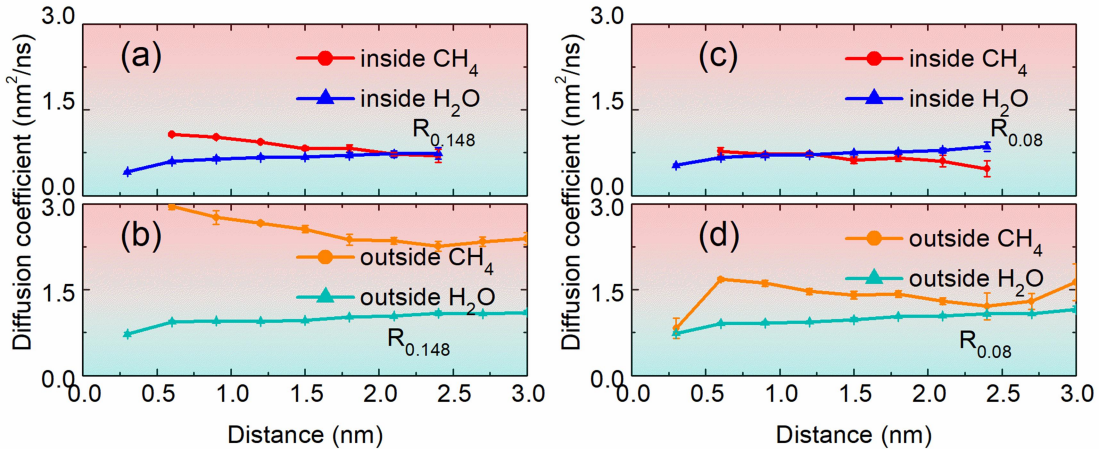


**Figure S7.** Diffusion coefficients ( $K_{DC}$ ) of  $\text{CH}_4/\text{H}_2\text{O}$  molecules at various radial distances from the inner and outer surfaces of the HNTs at the end of 20-ns adsorption simulation for the (a, b)  $R_{0.148}$  and (c, d)  $R_{0.08}$  simulation systems.

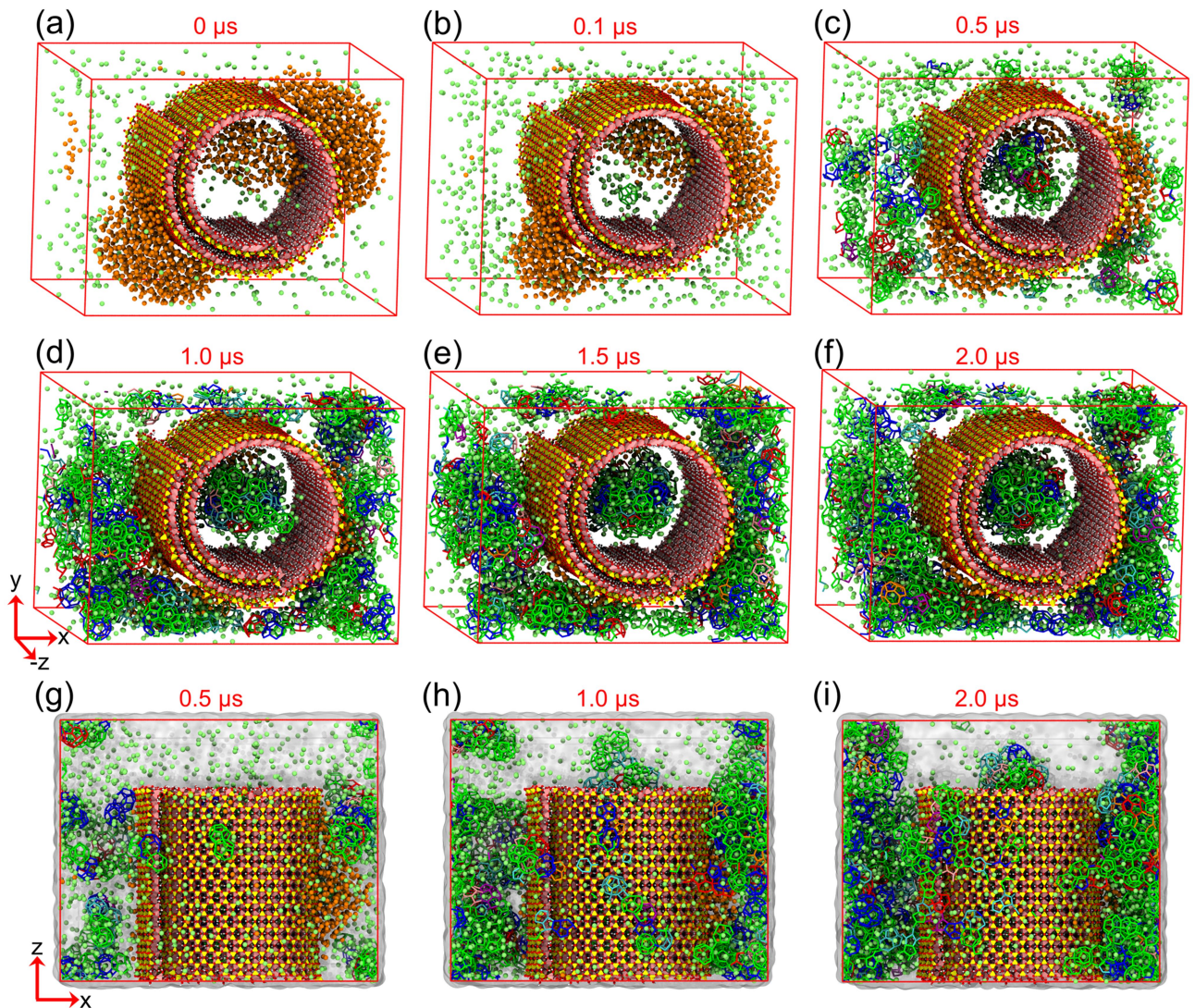


**Figure S8.** Formation processes of CH<sub>4</sub> hydrate inside and outside of the HNTs for the (a-i) R<sub>0.08</sub> simulation system. The HNT is displayed as polyhedral, *i.e.* yellow (Si atom) and pink (Al atom). Orange and green balls represent CH<sub>4</sub> molecules in nanobubble and solution, respectively. Hydrate cages are shown as sticks in various colors (green for 5<sup>12</sup>, blue for 5<sup>12</sup>6<sup>2</sup>, red for 5<sup>12</sup>6<sup>3</sup>, orange for 5<sup>12</sup>6<sup>4</sup>, cyan for 4<sup>1</sup>5<sup>10</sup>6<sup>2</sup>, purple for 4<sup>1</sup>5<sup>10</sup>6<sup>3</sup> and pink for 4<sup>1</sup>5<sup>10</sup>6<sup>4</sup>).

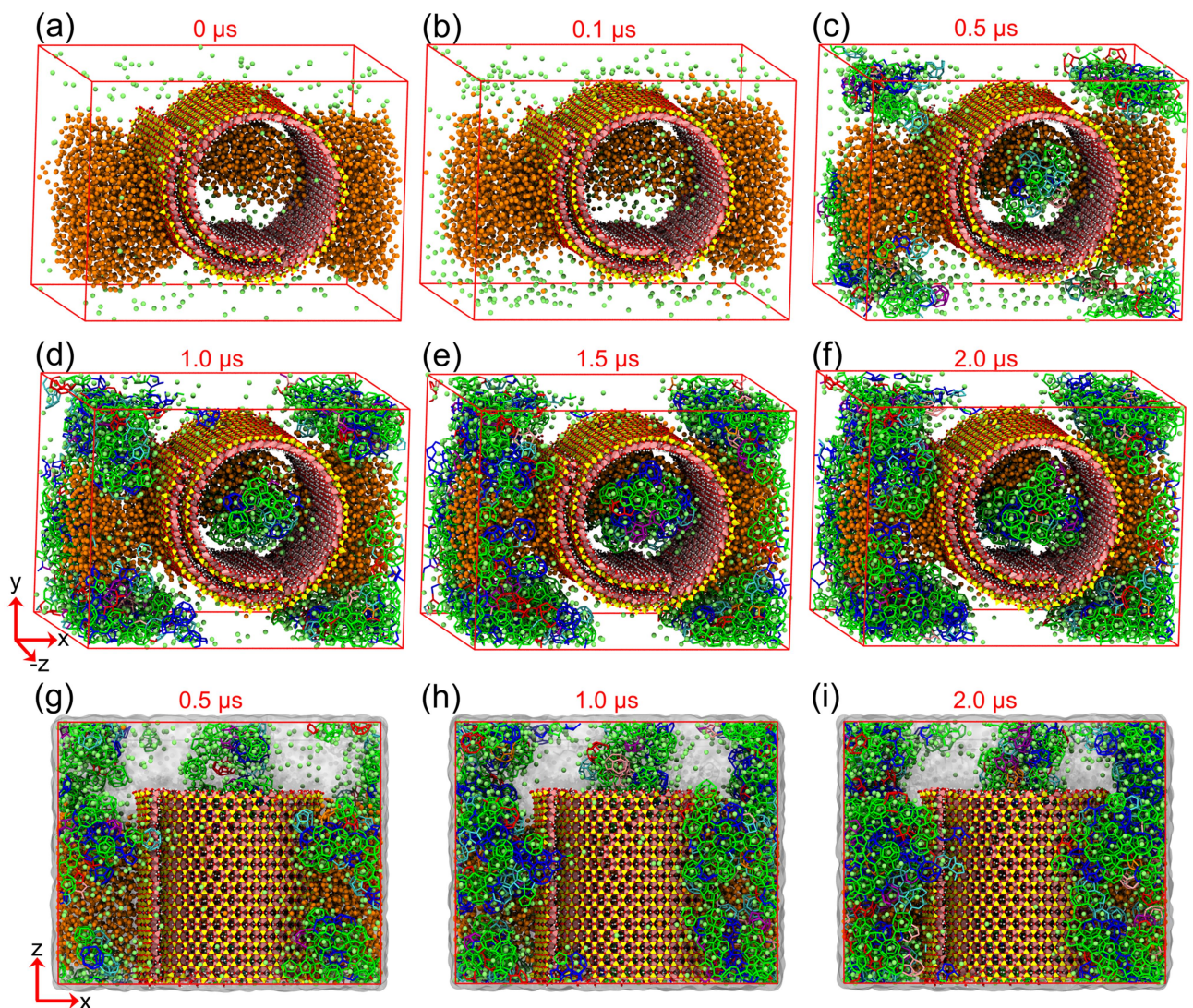


**Figure S9.** Formation processes of CH<sub>4</sub> hydrate inside and outside of the HNTs for the (a-i) R<sub>0.148</sub> simulation system. The HNT is displayed as polyhedral, *i.e.* yellow (Si atom) and pink (Al atom). Orange and green balls represent CH<sub>4</sub> molecules in nanobubble and solution, respectively. Hydrate cages are shown as sticks in various colors (green for 5<sup>12</sup>, blue for 5<sup>12</sup>6<sup>2</sup>, red for 5<sup>12</sup>6<sup>3</sup>, orange for 5<sup>12</sup>6<sup>4</sup>, cyan for 4<sup>1</sup>5<sup>10</sup>6<sup>2</sup>, purple for 4<sup>1</sup>5<sup>10</sup>6<sup>3</sup> and pink for 4<sup>1</sup>5<sup>10</sup>6<sup>4</sup>).

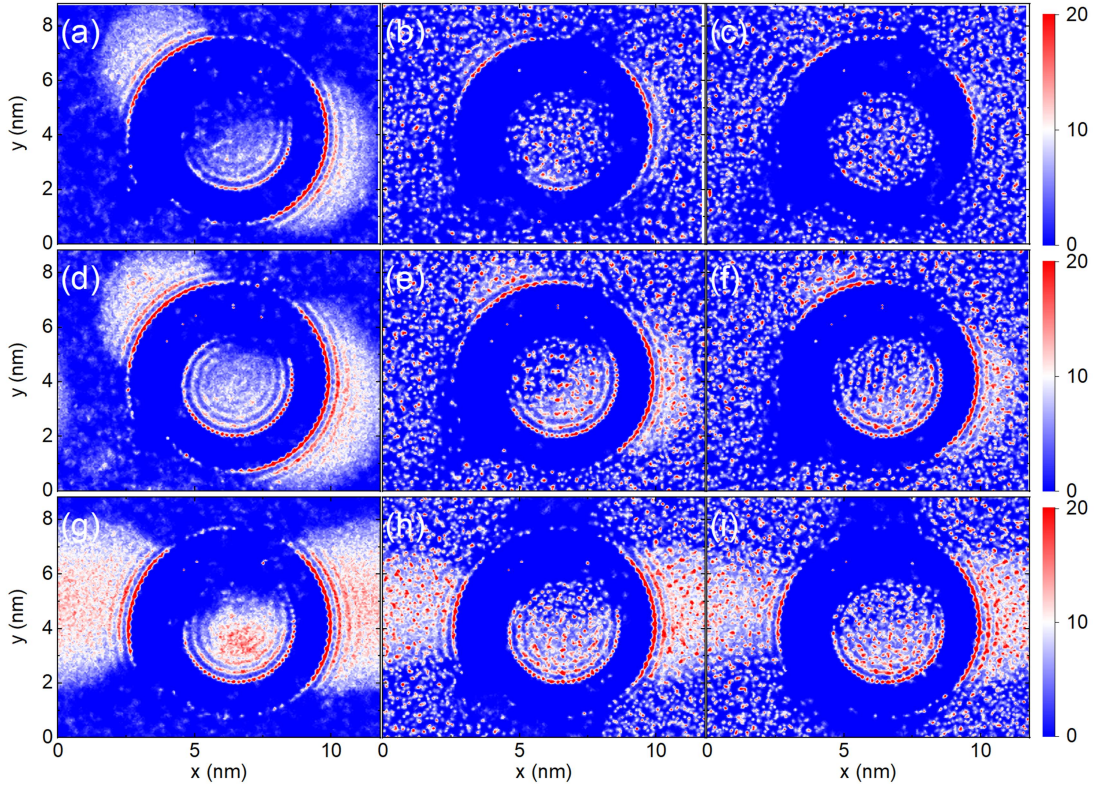


**Figure S10.** Number density distribution of  $\text{CH}_4$  molecules for the last  $0.001 \mu\text{s}$  in the three simulation systems *i.e.* (a-c)  $\text{R}_{0.08}$ , (d-f)  $\text{R}_{0.12}$ , (g-i)  $\text{R}_{0.148}$  simulation systems.

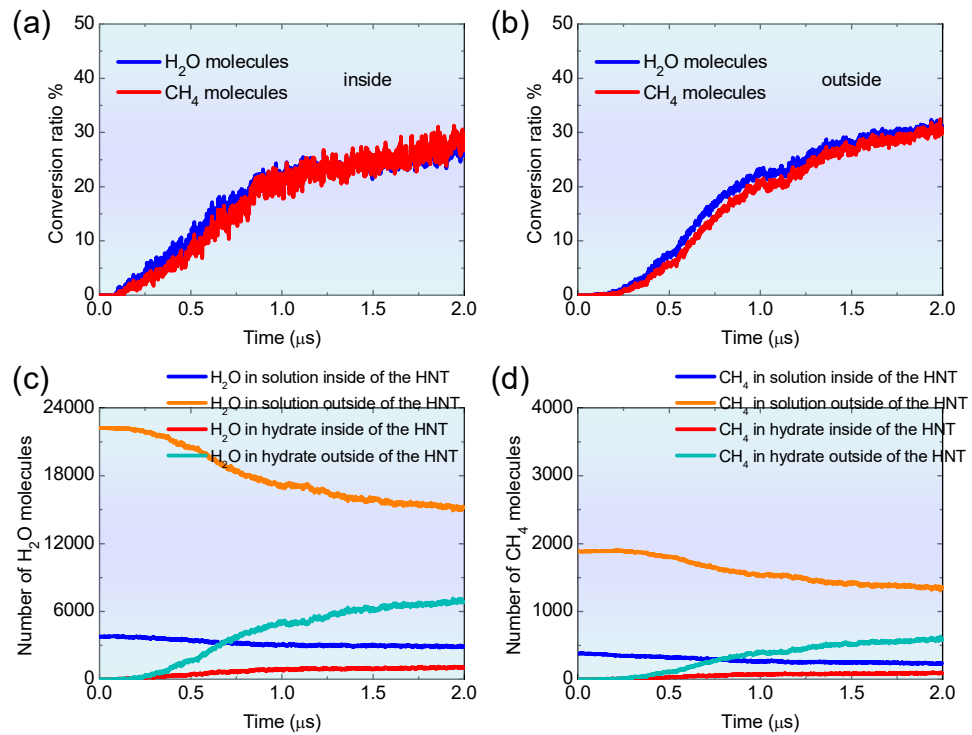


**Figure S11.** The evolution of the (a-b) conversion ratio of  $\text{CH}_4/\text{H}_2\text{O}$  molecules and (c-d) number of  $\text{CH}_4/\text{H}_2\text{O}$  molecules in solution and hydrate inside and outside of the HNTs for the  $\text{R}_{0.08}$  simulation system. Conversion ratio is defined as the number of  $\text{CH}_4/\text{H}_2\text{O}$  in hydrate divided by the total number.

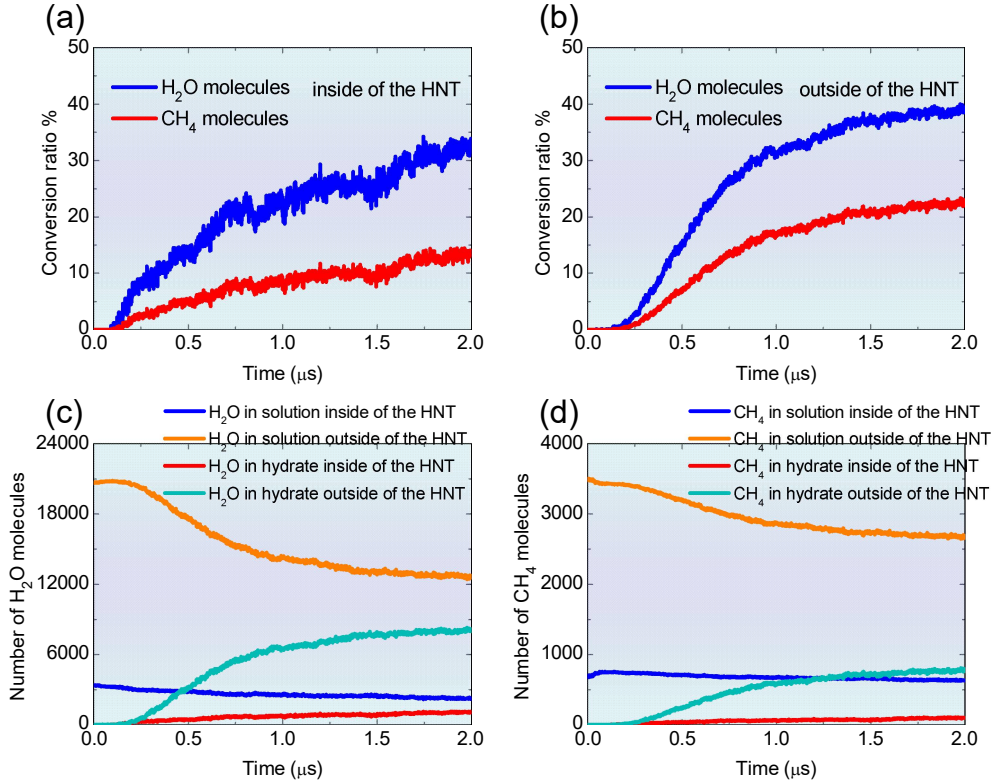


**Figure S12.** The evolution of the (a-b) conversion ratio of CH<sub>4</sub>/H<sub>2</sub>O molecules and (c-d) number of CH<sub>4</sub>/H<sub>2</sub>O molecules in solution and hydrate inside and outside of the HNTs for the R<sub>0.148</sub> simulation system. Conversion ratio is defined as the number of CH<sub>4</sub>/H<sub>2</sub>O in hydrate divided by the total number.

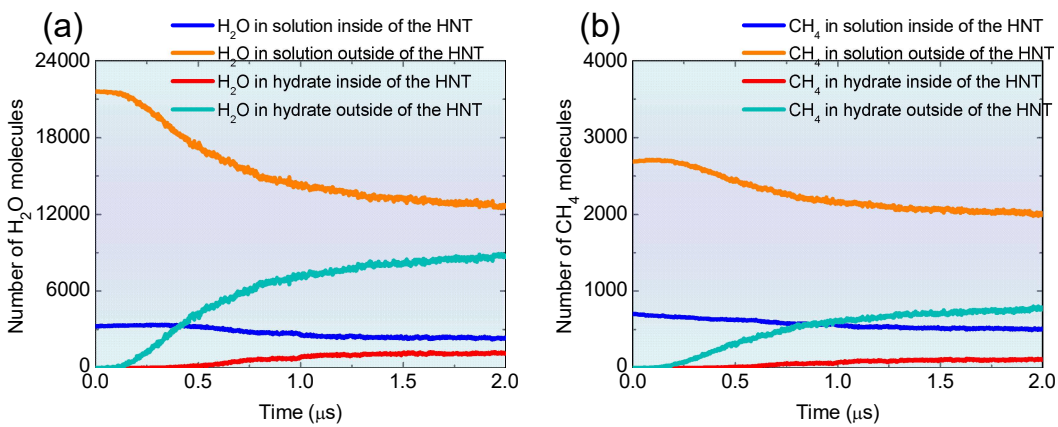


**Figure S13.** The evolution of the number of (a) H<sub>2</sub>O and (b) CH<sub>4</sub> molecules in solution and hydrate for the R<sub>0.12</sub> simulation system.

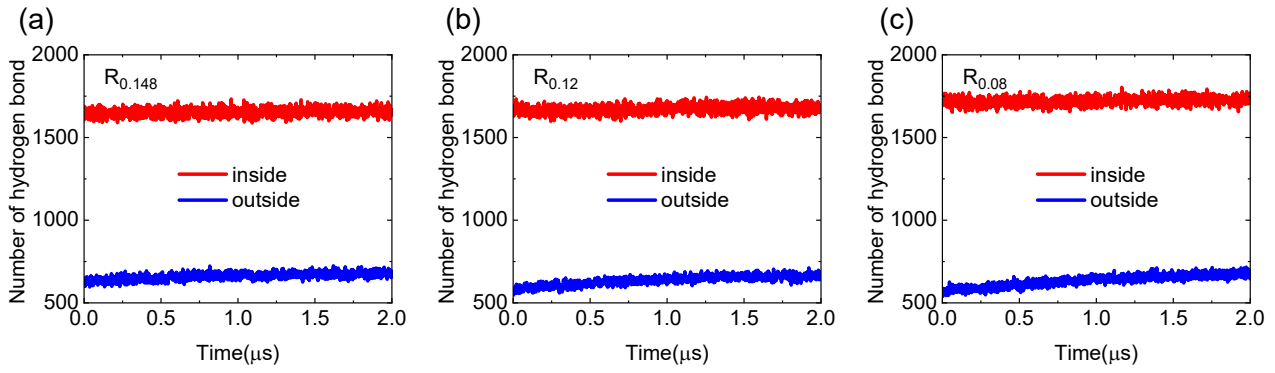


**Figure S14.** The evolution of the number of hydrogen bonds between water molecules and both the inner and outer surfaces of the HNTs for the (a)  $R_{0.148}$ , (b)  $R_{0.12}$ , and (c)  $R_{0.08}$  simulation systems.

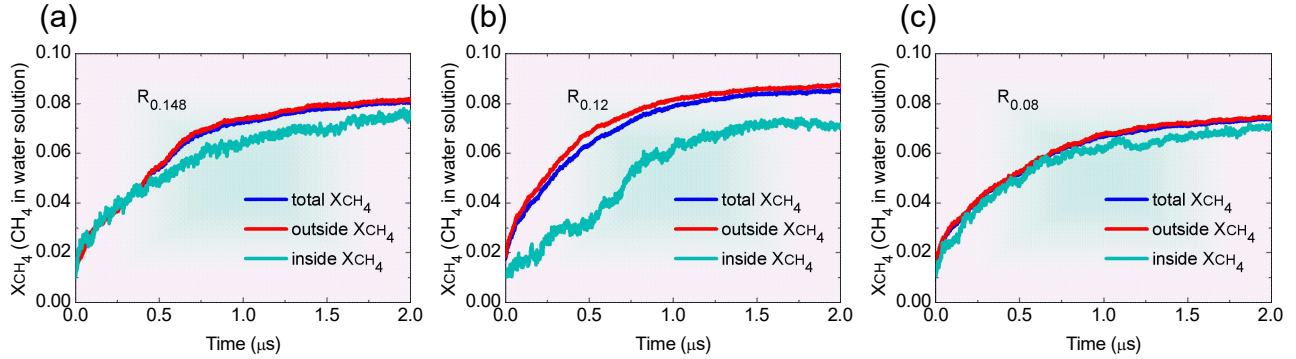


**Figure S15.** The evolution of the  $\text{CH}_4$  mole fraction in water  $x_{\text{CH}_4}$  inside and outside of the HNTs and total for the (a)  $R_{0.148}$ , (b)  $R_{0.12}$ , and (c)  $R_{0.08}$  simulation systems.

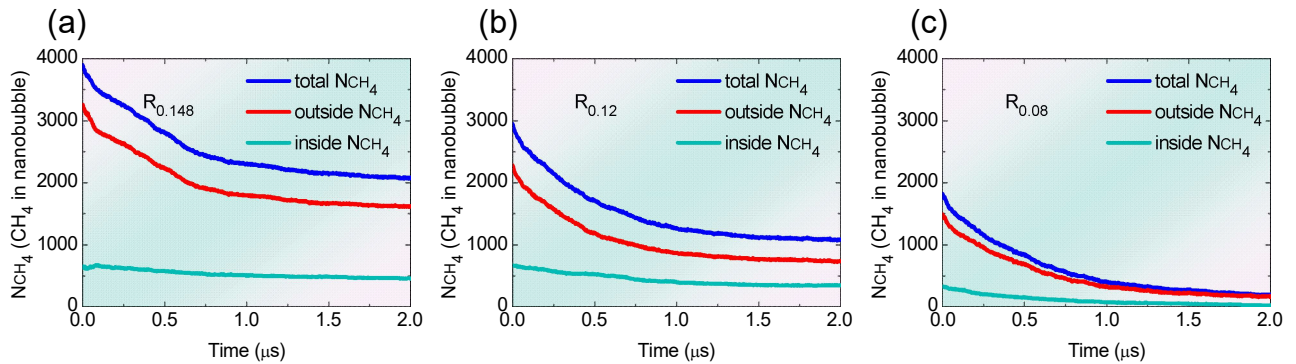


**Figure S16.** The evolution of the  $\text{CH}_4$  in the nanobubbles  $N_{\text{CH}_4}$  inside and outside of the HNTs and total for the (a)  $R_{0.148}$ , (b)  $R_{0.12}$ , and (c)  $R_{0.08}$  simulation systems.

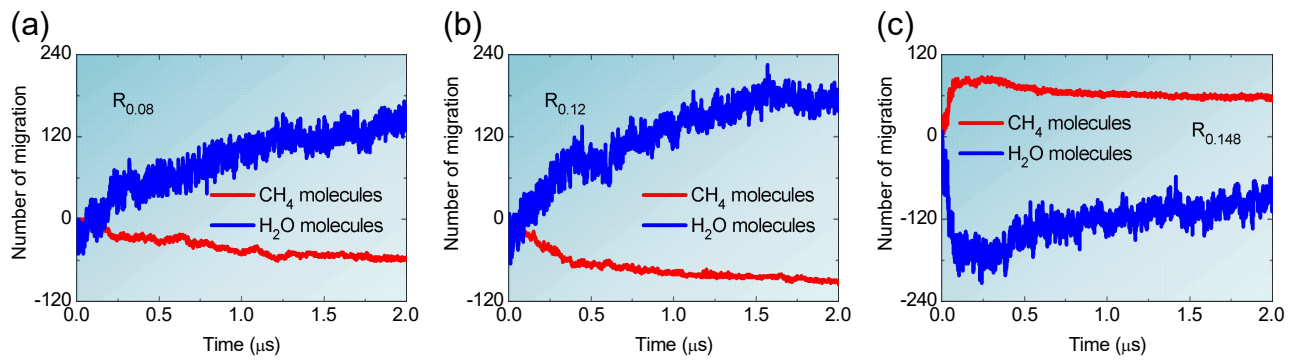


**Figure S17.** The evolution of the number of CH<sub>4</sub>/H<sub>2</sub>O molecules migration from inside to outside of the HNTs for the (a) R<sub>0.08</sub>, (b) R<sub>0.12</sub>, and (c) R<sub>0.148</sub> simulation systems.

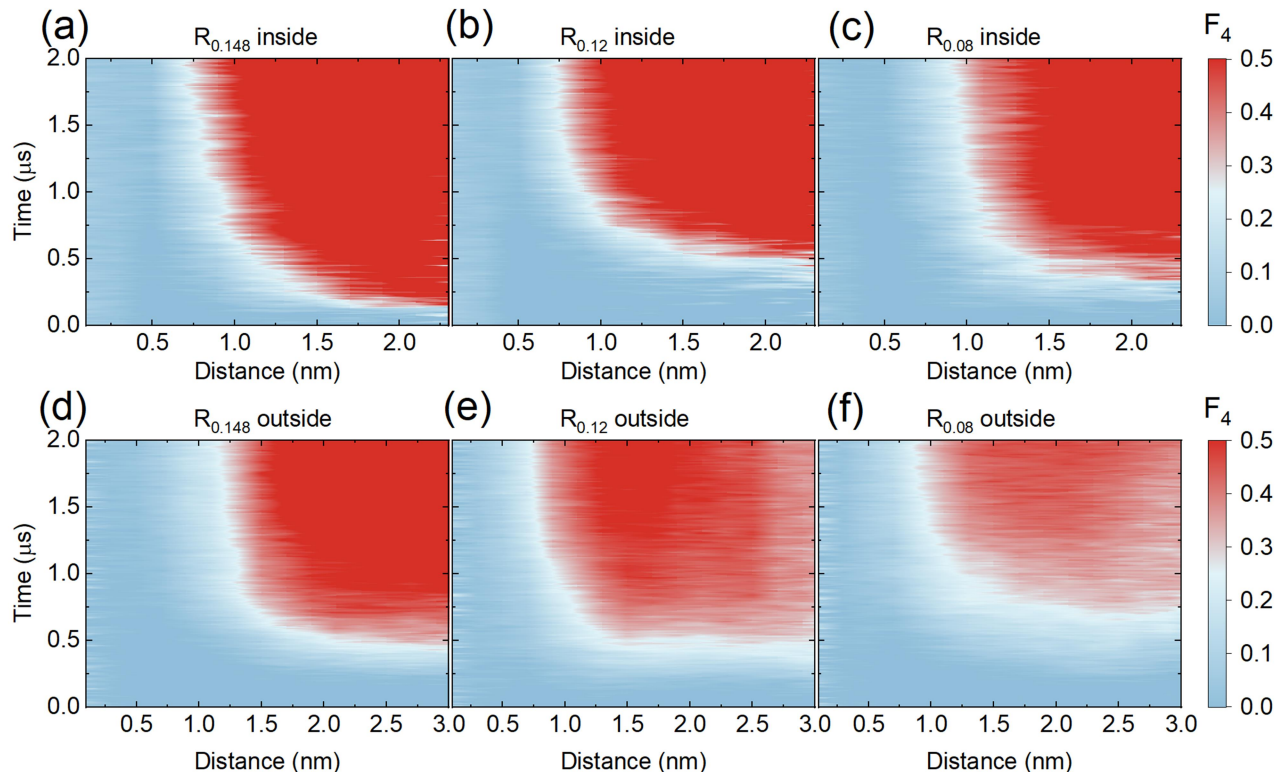


**Figure S18.** The evolution of the  $F_4$  order parameter under the different radial distances from the inner and outer surfaces of the HNTs for the (a, d) R<sub>0.148</sub>, (b, e) R<sub>0.12</sub>, and (c, f) R<sub>0.08</sub> simulation systems.

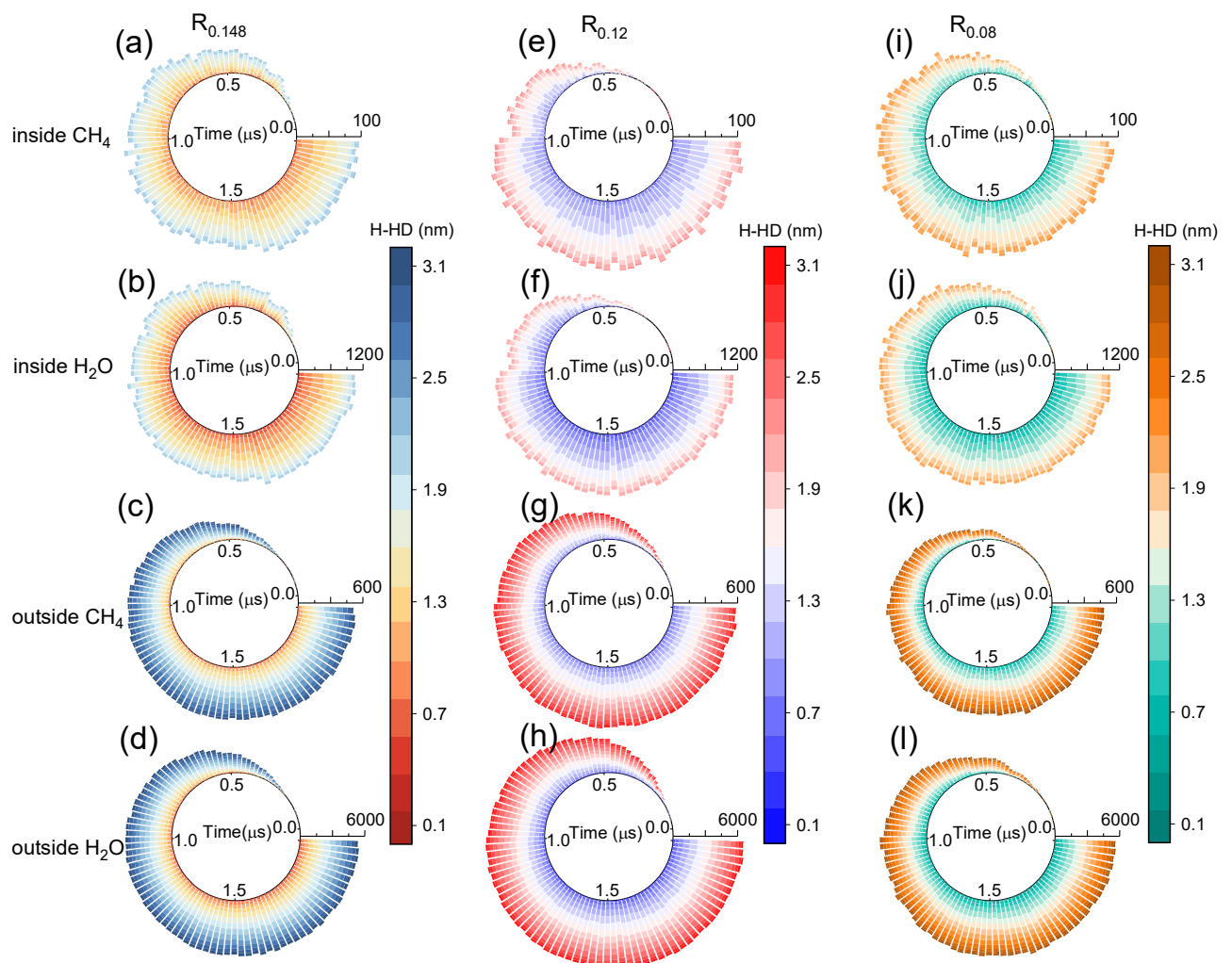


**Figure S19.** The evolution of the number of CH<sub>4</sub>/H<sub>2</sub>O molecules in hydrate as a function of the radial distances from the inner and outer surfaces of the HNTs for the (a-d) R<sub>0.148</sub>, (e-h) R<sub>0.12</sub>, and (i-l) R<sub>0.08</sub> simulation systems. These values were calculated for each 20ns.

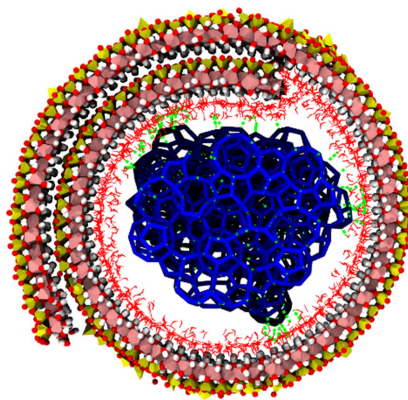


**Figure S20.** The snapshot of the hydrogen bonds (green lines) between the bound water on the inner surface and the hydrate solids inside of the HNTs at 2.0- $\mu$ s for the (a-i) R<sub>0.08</sub> simulation system. The HNT is displayed as polyhedral, *i.e.* yellow (Si atom) and pink (Al atom). Blue bonds represent hydrate solids inside of the HNTs.

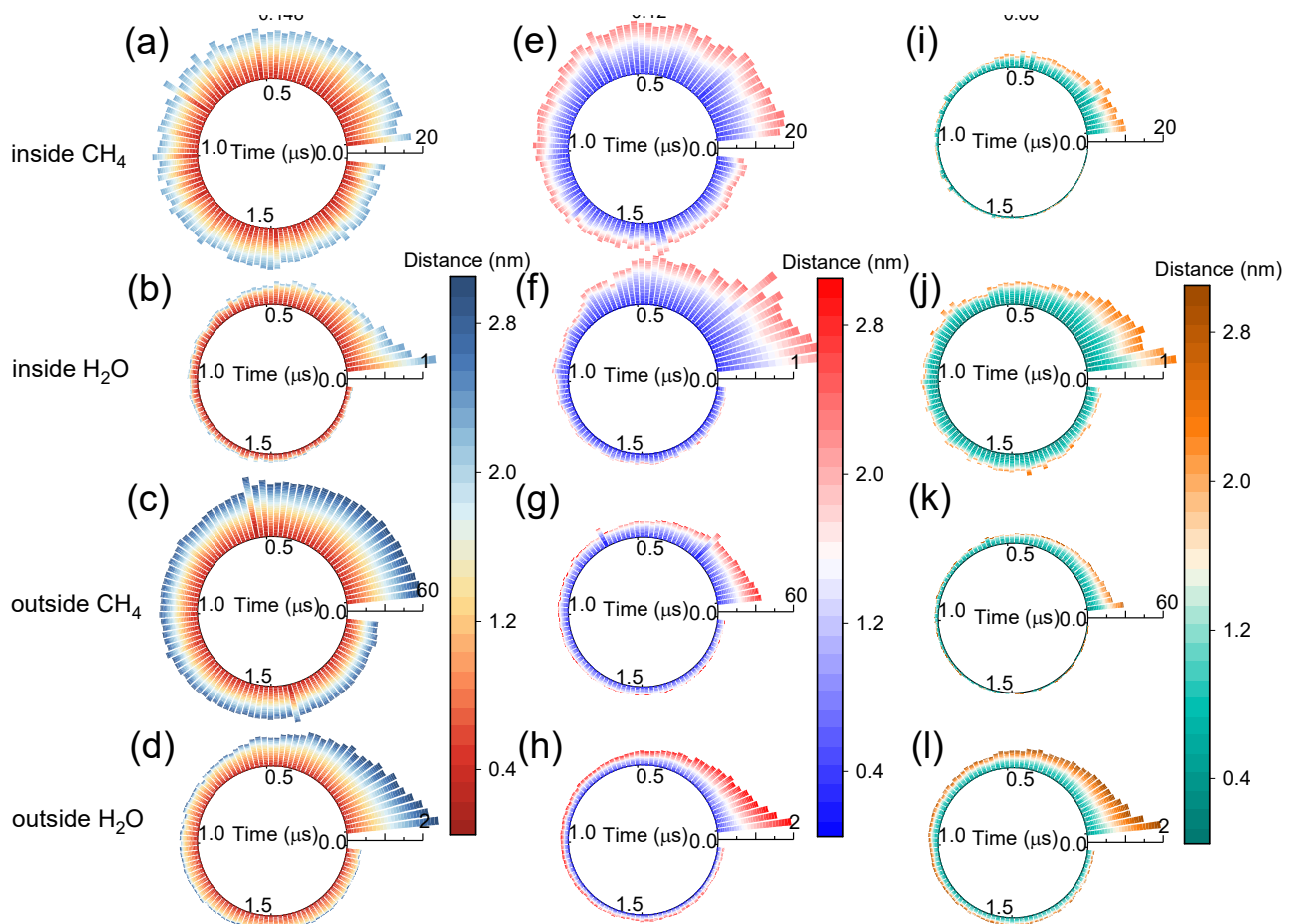


**Figure S21.** The evolution of the diffusion coefficient ( $K_{DC}$ ) of CH<sub>4</sub>/H<sub>2</sub>O molecules as a function of the radial distances from the inner and outer surfaces of the HNTs for the (a-d) R<sub>0.148</sub>, (e, h) R<sub>0.12</sub>, and (i-l) R<sub>0.08</sub> simulation systems. These values were calculated for each 20ns.

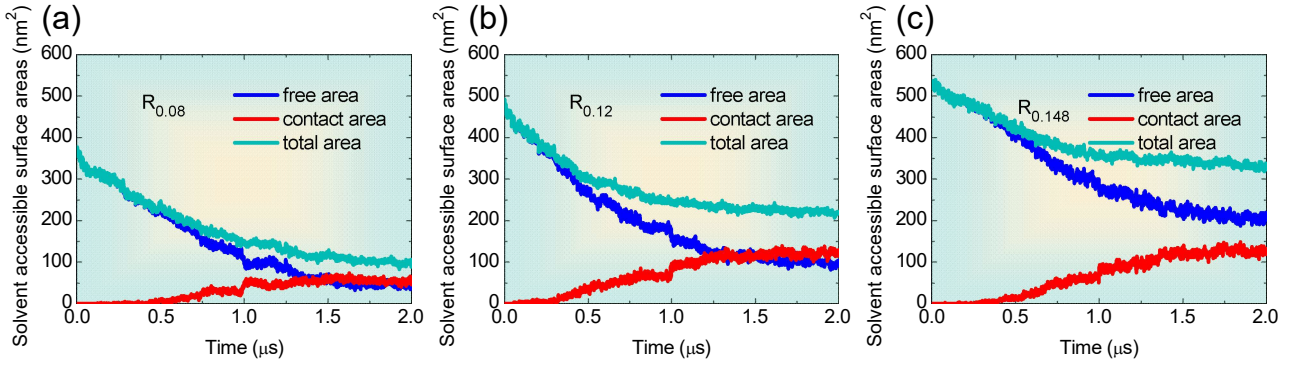


**Figure S22.** The evolution of the solvent accessible surface area of CH<sub>4</sub> nanobubbles for free, contact and total area in the (a) R<sub>0.08</sub>, (b) R<sub>0.12</sub>, and (c) R<sub>0.148</sub> simulation systems.

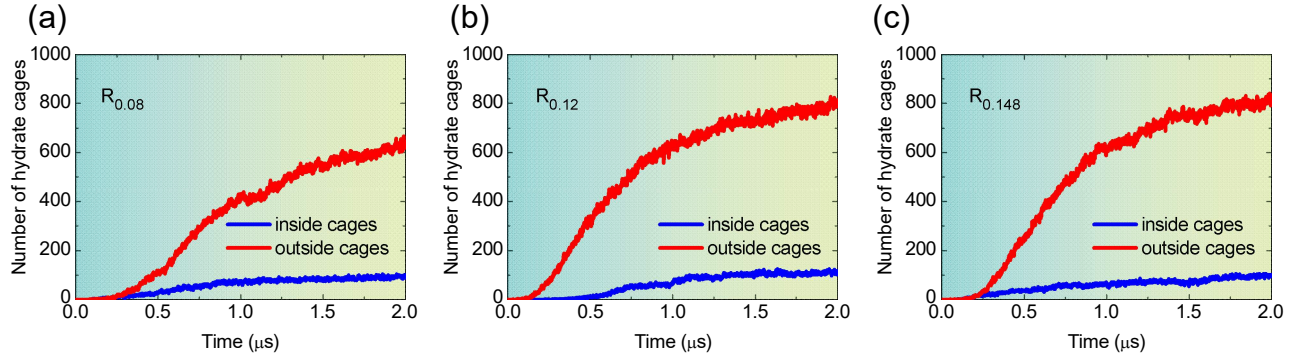


**Figure S23.** The evolution of the number of hydrate cages inside and outside of the HNTs for the (a) R<sub>0.08</sub>, (b) R<sub>0.12</sub>, and (c) R<sub>0.148</sub> simulation systems.

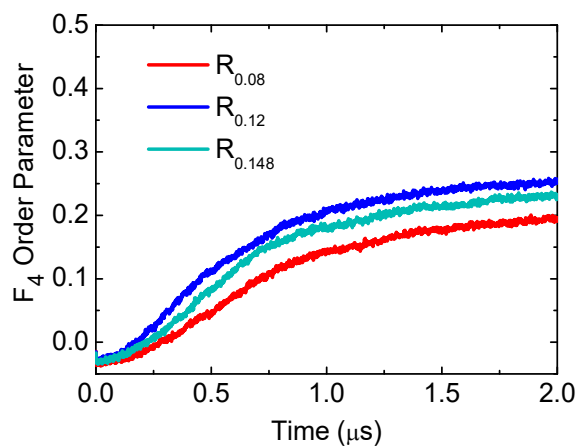


**Figure S24.** The evolution of the  $F_4$  order parameter for the R<sub>0.148</sub>, R<sub>0.12</sub>, and R<sub>0.08</sub> simulation systems.

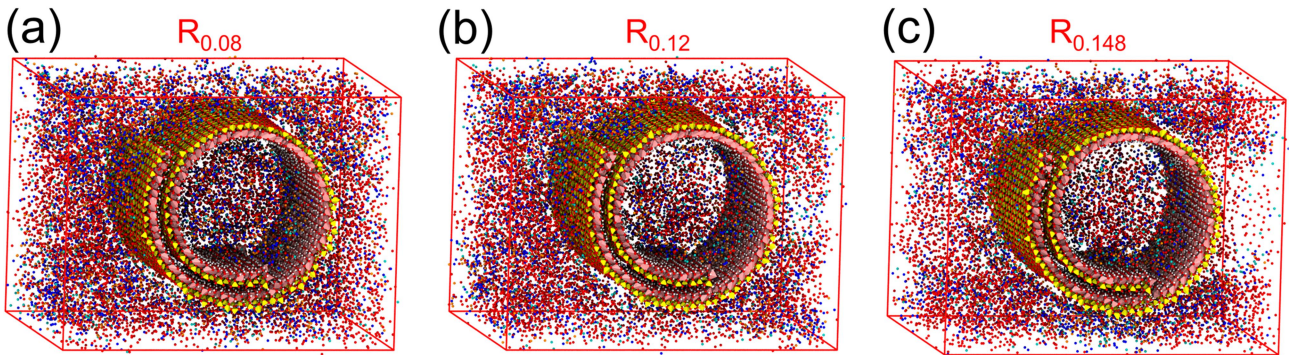


**Figure S25.** Snapshots of water ring inside and outside of the HNTs at 2  $\mu$ s (a-c) in the  $R_{0.08}$ ,  $R_{0.12}$  and  $R_{0.148}$  simulation systems. Cyan, red, blue and orange balls represent ring\_4, ring\_5, ring\_6 and ring\_7, respectively.

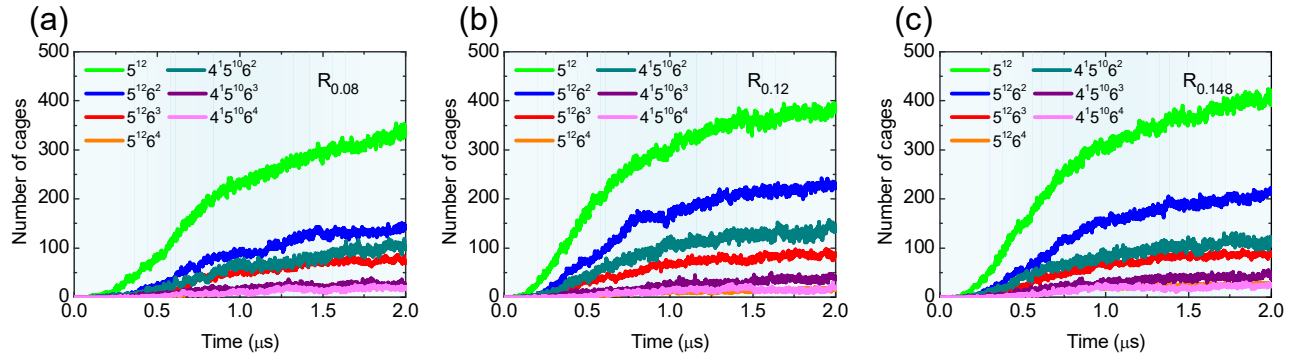


**Figure S26.** The evolution of the number of hydrate cages for the (a)  $R_{0.08}$ , (b)  $R_{0.12}$ , and (c)  $R_{0.148}$  simulation systems.

## Supporting Videos

**Video S1.** Adsorption processes of  $\text{CH}_4$  molecules inside and outside of the HNTs for the  $R_{0.08}$  simulation system. The HNTs are displayed as polyhedral, *i.e.* yellow (Si atom) and pink (Al atom). Green ball represents  $\text{CH}_4$  molecules.

**Video S2.** Adsorption processes of  $\text{CH}_4$  molecules inside and outside of the HNTs for the  $R_{0.12}$  simulation system. The HNTs are displayed as polyhedral, *i.e.* yellow (Si atom) and pink (Al atom). Green ball represents  $\text{CH}_4$  molecules.

**Video S3.** Adsorption processes of  $\text{CH}_4$  molecules inside and outside of the HNTs for the  $R_{0.148}$  simulation system. The HNTs are displayed as polyhedral, *i.e.* yellow (Si atom) and pink (Al atom). Green ball represents  $\text{CH}_4$  molecules.

**Video S4.** Formation processes of  $\text{CH}_4$  hydrates inside and outside of the HNTs for the  $R_{0.08}$  simulation system. The HNTs are displayed as polyhedral, *i.e.* yellow (Si atom) and pink (Al atom). Green ball represents  $\text{CH}_4$

molecules. Hydrate cages are shown as sticks in various colors (green for  $5^{12}$ , blue for  $5^{12}6^2$ , red for  $5^{12}6^3$ , orange for  $5^{12}6^4$ , cyan for  $4^15^{10}6^2$ , purple for  $4^15^{10}6^3$  and pink for  $4^15^{10}6^4$ ).

**Video S5.** Formation processes of CH<sub>4</sub> hydrates inside and outside of the HNTs for the R<sub>0.12</sub> simulation system. The HNTs are displayed as polyhedral, *i.e.* yellow (Si atom) and pink (Al atom). Green ball represents CH<sub>4</sub> molecules. Hydrate cages are shown as sticks in various colors (green for  $5^{12}$ , blue for  $5^{12}6^2$ , red for  $5^{12}6^3$ , orange for  $5^{12}6^4$ , cyan for  $4^15^{10}6^2$ , purple for  $4^15^{10}6^3$  and pink for  $4^15^{10}6^4$ ).

**Video S6.** Formation processes of CH<sub>4</sub> hydrates inside and outside of the HNTs for the R<sub>0.148</sub> simulation system. The HNTs are displayed as polyhedral, *i.e.* yellow (Si atom) and pink (Al atom). Green ball represents CH<sub>4</sub> molecules. Hydrate cages are shown as sticks in various colors (green for  $5^{12}$ , blue for  $5^{12}6^2$ , red for  $5^{12}6^3$ , orange for  $5^{12}6^4$ , cyan for  $4^15^{10}6^2$ , purple for  $4^15^{10}6^3$  and pink for  $4^15^{10}6^4$ ).

## Supporting Reference

- (1) Ferrante, F.; Armata, N.; Lazzara, G. Modeling of the Halloysite Spiral Nanotube. *J. Phys. Chem. C* **2015**, *119* (29), 16700-16707.
- (2) Lvov, Y. M.; Shchukin, D. G.; Mohwald, H.; Price, R. R. Halloysite clay nanotubes for controlled release of protective agents. *ACS nano* **2008**, *2* (5), 814-820.
- (3) Em, Y.; Stoporev, A.; Semenov, A.; Glotov, A.; Smirnova, E.; Villevald, G.; Vinokurov, V.; Manakov, A.; Lvov, Y. Methane Hydrate Formation in Halloysite Clay Nanotubes. *ACS Sustain Chem. Eng.* **2020**, *8* (21), 7860-7868.
- (4) Bussi, G.; Donadio, D.; Parrinello, M. Canonical sampling through velocity rescaling. *J Chem Phys* **2007**, *126* (1), 014101.
- (5) Berendsen, H. J. C.; Postma, J. P. M.; Vangunsteren, W. F.; Dinola, A.; Haak, J. R. Molecular-Dynamics with Coupling To an External Bath. *J. Chem. Phys.* **1984**, *81* (8), 3684-3690.
- (6) Abascal, J. L.; Sanz, E.; Garcia Fernandez, R.; Vega, C. A potential model for the study of ices and amorphous water: TIP4P/Ice. *J. Chem. Phys.* **2005**, *122* (23), 234511.
- (7) Jorgensen, W. L.; Madura, J. D.; Swenson, C. J. Optimized Intermolecular Potential Functions for Liquid Hydrocarbons. *J. Am. Chem. Soc.* **1984**, *106* (22), 6638-6646.
- (8) Cygan, R. T.; Liang, J. J.; Kalinichev, A. G. Molecular models of hydroxide, oxyhydroxide, and clay phases and the development of a general force field. *J. Phys. Chem. B* **2004**, *108* (4), 1255-1266.